VIP *Very Important Paper*

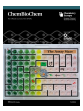

Assessing Lanthanide-Dependent Methanol Dehydrogenase Activity: The Assay Matters

Manh Tri Phi,[a] Helena Singer,[a] Felix Zäh,[a] Christoph Haisch,[b] Sabine Schneider,[a] Huub J. M. Op den Camp,[c] and Lena J. Daumann*[a, d]

Artificial dye-coupled assays have been widely adopted as a rapid and convenient method to assess the activity of methanol dehydrogenases (MDH). Lanthanide(Ln)-dependent XoxF-MDHs are able to incorporate different lanthanides (Lns) in their active site. Dye-coupled assays showed that the earlier Lns exhibit a higher enzyme activity than the late Lns. Despite widespread use, there are limitations: oftentimes a pH of 9 and activators are required for the assay. Moreover, Ln-MDH variants are not obtained by isolation from the cells grown with the respective Ln, but by incubation of an apo-MDH with the Ln. Herein, we report the cultivation of Ln-dependent methanotroph *Methylacidiphilum fumariolicum* SolV with nine different Lns, the isolation of the respective MDHs and the assessment of the enzyme activity using the dye-coupled assay. We compare these results with a protein-coupled assay using its physiological electron acceptor cytochrome c_{GJ} (cyt c_{GJ}). Depending on the assay, two distinct trends are observed among the Ln series. The specific enzyme activity of La-, Ce- and Pr-MDH, as measured by the protein-coupled assay, exceeds that measured by the dye-coupled assay. This suggests that early Lns also have a positive effect on the interaction between XoxF-MDH and its cyt c_{GJ} thereby increasing functional efficiency.

Introduction

In recent years, lanthanides (Ln, La–Lu) have firmly been established as biological relevant. Ln-dependent or -utilizing bacteria have been found in a variety of ecosystems, e.g. phyllosphere, pond sediment, (coastal) marine environment, shale rock, rice rhizosphere and geothermal fields.[1] Most of these bacteria are either methylotrophs or methanotrophs and use small C_1-molecules like methane, methanol, halogenated methanes, methylated amines and methylated sulfur species as their energy source.[2] Methanotrophs are able to convert methane to carbon dioxide and play a significant role in the global carbon cycle.[1c] In the first step, methane is oxidized to methanol by particulate methane monooxygenase or soluble methane monooxygenase and subsequently oxidized to formaldehyde by methanol dehydrogenase (MDH).[3] There are two variants of this MDH: Ca-containing MxaFI-MDH and Ln-containing XoxF-MDH. All methanotrophs that possess the MxaFI-MDH variant also have the XoxF-MDH.[2,4] There are also reports of methano- and methylotrophs that exclusively possess the XoxF-MDH, highlighting the widespread prevalence of Ln-utilizing microorganisms.[1g,5]

If both types of MDH are present, MxaFI-MDH is expressed in the absence of any Ln. However, even the presence of nanomolar amounts of Ln is sufficient to initiate a transcriptional response, the "lanthanide-switch", favouring the expression of the XoxF-MDH variant even when the concentration of Ca is 100-fold higher.[9] In addition to the Ln ion, the active site contains pyrroloquinoline quinone (PQQ) as the second essential cofactor for XoxF-MDH (Figure 1).[6]

The mechanistic details of methanol oxidation by XoxF-MDH remains up for debate but two mechanisms are widely discussed by "wet-lab" and computational research groups: the addition-elimination and hydride transfer mechanism.[7,10] Pol *et al.* isolated the acidophilic methanotroph *Methylacidiphilum fumariolicum* SolV from a volcanic mudpot.[6] This bacterium is strictly dependent on Ln and exclusively possesses XoxF-MDH.[6,11] To cultivate SolV in a laboratory set-up, the extreme conditions of its natural environment have to be provided, including a Ln source, high temperature, low pH and the supply of methane and carbon dioxide.[6,12]

Most, if not all methylotrophic bacteria contain two distinct periplasmic, c-type cytochromes known as c_L and c_H. In the past, these cytochromes were designated based on their isoelectric points (p*I*), cyt c_L having the lower p*I* value and cyt c_H the higher

[a] *M. T. Phi, H. Singer, F. Zäh, Dr. S. Schneider, Prof. Dr. L. J. Daumann*
Department of Chemistry
Ludwig-Maximilians-Universität München
Butenandtstr. 5–13, 81377 München (Germany)
[b] *Prof. Dr. C. Haisch*
Faculty of Chemistry
Technical University of Munich
Lichtenbergstr. 4, 85748 Garching (Germany)
[c] *Prof. H. J. M. Op den Camp*
Department of Microbiology
Research Institute for Biological and Environmental Sciences
Radboud University Nijmegen
Heyendaalseweg 135, 6525 AJ, Nijmegen (The Netherlands)
[d] *Prof. Dr. L. J. Daumann*
Chair of Bioinorganic Chemistry
Heinrich-Heine-Universität Düsseldorf
Universitätsstraße 1, 40225 Düsseldorf (Germany)
E-mail: lena.daumann@hhu.de

Supporting information for this article is available on the WWW under https://doi.org/10.1002/cbic.202300811

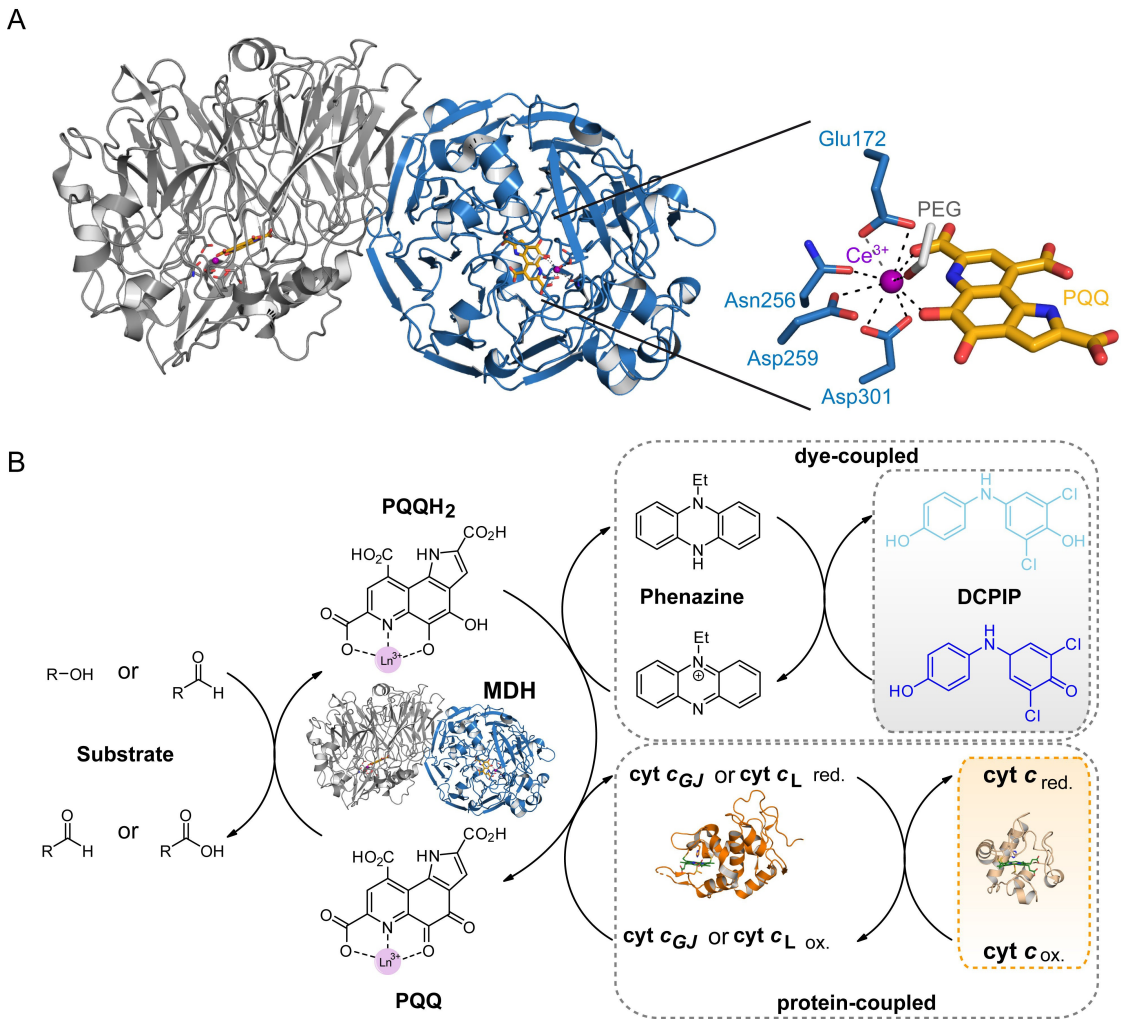

Figure 1. A) Homodimeric structure of Ce-MDH from *Methylacidiphilum fumariolicum* SolV (PDB: 4MAE)[6] and zoom in its active center. The cofactors PQQ and Ce^{3+}, as well as the coordinating amino acids are highlighted. The substrate binding coordination position of the Ce^{3+} is occupied by a polyethylene glycol (PEG) molecule from the crystallization buffer. (B) Schematic overview of the dye- and protein-coupled assay used in this study. Phenazine ethosulfate is reduced by $PQQH_2$ in MDH, leading to the reduction of DCPIP and causing its discoloration. $PQQH_2$ also reduces cyt c_{GJ} which in turn reduces equine heart cyt *c*. The change in absorbance for DCPIP and equine heart cyt *c* can be measured using UV/Vis at A_{600} and A_{550}, respectively. The crystal structures of cytochrome c XoxG from *Methylorubrum extorquens* AM1 (PDB: 6ONQ) and equine heart cyt *c* (PDB: 1HRC) were used to illustrate this scheme. PQQ, pyrroloquinoline quinone. $PQQH_2$, pyrroloquinoline quinol. DCPIP, 2,6-dichlorophenolindophenol. Modified from Refs. [7] and [8].

value. Only the cyt c_L is able to interact with MDH.[13] The physiological electron transfer of MxaFI-MDH from substrate to its immediate cyt c_L was extensively studied by Anthony and co-workers in *Methylorubrum extorquens* AM1.[14] Fundamentally, oxidation of methanol results in a concomitant reduction of PQQ to $PQQH_2$, which is step-wise re-oxidized after two single electron transfers to two separate molecules of cyt c_L which is reduced as well. Finally, cyt c_L regeneration is achieved through an additional electron transfer to cyt c_H.[13] In case of SolV, cyt c_L is termed cyt c_{GJ} and consists of the XoxG cytochrome and a periplasmic binding protein XoxJ.[15] The interaction or "docking" of cyt c_{GJ} to XoxF-MDH involves electrostatic interaction between lysine residues on XoxF-MDH and carboxyl residues on cyt c_{GJ}. Disassembly of the reduced cyt c_{GJ} is required before XoxF-MDH can interact with the next molecule of cyt c_{GJ}. Electrostatic interactions are also involved for the electron transfer from cyt c_{GJ} to cyt c_H.[14a] The interaction between XoxF-MDH and cyt c_{GJ} is disturbed by high salt concentration which inhibits substrate oxidation by up to 50% at 150 mM NaCl, 100 mM K_2SO_4 or 25 mM phosphate.[14a,15] Furthermore, electrochemical experiments revealed that cyt c_{GJ} itself exhibits temperature dependence, with a 20% increase in current going from 10 to 35 °C.[16] Featherston *et al.* characterized the immediate cytochrome of XoxF-MDH, XoxG, from *M. extorquens* AM1 (the structure of this cytochrome is shown in Figure 1B in lieu of a structure of the native electron acceptor from SolV). By comparing the results of an artificial dye-coupled assay with a XoxG-based assay, they concluded that these assays measure distinct aspects of XoxF-MDH activity.[17]

For decades, the most commonly practiced method to determine the activity of MDHs is a dye-coupled assay using the dyes phenazine ethosulfate (PES) as primary and 2,6-dichlorophenolindophenol (DCPIP) as secondary artificial electron acceptor.[18] The reduction of DCPIP results in its discolor-

ation which is measured at 600 nm by UV/Vis. Based on previous work by Anthony and co-workers, protein-coupled activity assays for MDH from SolV using its physiological cyt c_{GJ} partner were developed.[8,15,19] Commercially available cyt *c* from equine or bovine heart is used as secondary electron acceptor.[15] Again, the reduction of the secondary electron acceptor can be monitored to determine the enzyme activity (Figure 1B). Kalimuthu *et al.* developed an electrochemical assay that allows the co-adsorption of Eu-MDH and cyt c_{GJ} onto an electrode which functions as the secondary electron acceptor. In this case, the enzyme activity is tracked by measuring the current.[16]

Previous studies mainly used the dye-coupled assay to determine the enzyme activity of XoxF-MDH because the reagents are commercially available and low-cost. Usually a pH of 9, additives and activators like ammonia, glycine ethyl ester, potassium cyanide and an excess of Ln are included in the assay mixture to optimize the conditions for the assays (these additives are not necessary for MDH from *M. fumariolicum* SolV).[8] These experimental conditions rarely reflect the physiological conditions inside the cell and are truly artificial. Furthermore, the source of the endogenous substrate that causes background reaction is still unknown.[19] Although, Featherston *et al.* compared the enzyme activity of La-, Ce- and Pr-MDH from *M. extorquens* AM1 with the dye-coupled and protein-coupled assay, the differences in buffer, pH and activator do not allow for a direct comparison.[17]

Herein, we report the cultivation of *M. fumariolicum* SolV with nine different Lns and the isolation and purification of the respective Ln-MDHs and their physiological electron acceptor cyt c_{GJ}. Using the dye- and protein-coupled assays under the same assay conditions, we evaluated the enzyme activity of the different Ln-MDHs and observed varying trends among them, depending on the assay used.

Results and Discussion

The growth rate of *M. fumariolicum* SolV is highly dependent on supplemented Ln and its concentration in the growth medium.[6,12a] Compared to the growth of SolV with early Lns La-Nd, the growth rate of SolV with late lanthanide Gd is less than half.[6] When given a mixture of equimolar amount of all Ln and two actinides (Am, Cm), SolV preferably takes up the early Ln, showing the highest (80%) depletion from the medium for La.[12a] The depletion of Gd is barely 20% which is less than Am and Cm with a depletion of around 45% each.[12a] Based on the availability, XoxF-MDH is capable to incorporate a variety of Ln in its active site to obtain the respective Ln-MDH. We conducted nine separate cultivations of SolV at 55 °C and pH 2.7 with nine different Ln (La, Ce, Pr, Nd, Sm, Eu, Gd, Tb and Lu) in a self-build customized 3.5 L bioreactor, following a previously reported protocol.[12b] We observed exponential growth for seven out of nine cultivations (Figure S1) and stopped the cultivation of SolV with Tb and Lu after 10 days as only linear growth was observed with these elements. Nonetheless, cells of all cultivations were collected for isolation of XoxF-MDHs and cyt c_{GJ}. MDH makes up a high proportion of SolV's biomass and can be isolated without an affinity tag as previously shown.[6] The quantity of cyt c_{GJ} obtained after purification is low and makes native purification laborious. The heterologous expression of cyt c_{GJ} is desirable, but due to a so far unknown modification of or near its heme complex, native purification is, to the best of our knowledge, the only way to obtain cyt c_{GJ}.[15] Native protein purification of XoxF-MDHs and cyt c_{GJ} were performed by ion exchange chromatography and cyt c_{GJ} was additionally purified by size exclusion chromatography (SEC) (Figure S2). The addition of 1 mM MeOH to all buffer solutions is imperative to ensure stability and activity of Ln-MDHs along the purification process and for long-term storage.[6] To avoid secondary interactions of cyt c_{GJ} with the silica matrix, NaCl is added to the buffer for SEC. However, since the interaction of MDH and cyt c_{GJ} is mainly electrostatically and thus negatively affected by high salt concentrations, NaCl needs to be removed after SEC, which was done using centrifugal filter devices.[15] Ln-MDHs and cyt c_{GJ} were analyzed by SDS-PAGE (Figure S3) and the metal content of all Ln-MDHs was measured by Inductively Coupled Plasma Mass Spectrometer (ICP-MS).

ICP-MS measurement does not provide information about the metalation of the active site but rather the metal content of the sample. This can pose a challenge when XoxF-MDH co-purifies with other Ln-binding proteins such as LanM rendering the read-out ineffective, as noted by Featherston *et al.*[17] SolV does not encode LanM in its genome and the use of time-resolved laser-induced fluorescence spectroscopy (TRLFS) enables the differentiation between Eu in the active site and in solution. TRLFS confirms the previously determined metal content value of Eu-MDH obtained by ICP-MS analysis.[20] Previous studies found that XoxF-MDH from SolV is metallated on average with 60–70% of the respective Ln ions after purification.[6–7,20] Our results show that the metal content of Ln-MDH is higher in the case of early Lns (La–Nd), ranging from 42–48%. However, there is a notable decrease in metalation across the Ln series, with Tb-MDH having 11% metal content. La-XoxF1 from *M. extorquens* AM1 with a metal content of 39% displayed only half the specific activity compared to its previous studies.[21] As the metal content is highly variable depending on the batch and metal, we recommend to determine the metal content of Ln-MDHs, before conducting any experiment to ensure accurate and reliable data. Despite their similar ionic radii, these small differences influence the incorporation efficiency and retention of the Ln in the active site. MDH obtained from SolV grown with Lu did not contain detectable amounts of Lu and was omitted for further experiments. PQQ is the second indispensable cofactor in the active site of Ln-MDH. The occupancy of the cofactor was determined by measuring its absorption maximum at 355 nm.[7,10a] The cofactor was present in all samples but whether the loading is 100% cannot be taken from this method. Fully accounting for PQQ and/or metal contents continues to pose a challenge. Despite ongoing efforts, a comprehensive understanding of the exact mechanisms and factors influencing the presence and quantity of PQQ and/or metals remains elusive.

With eight Ln-MDHs and cyt c_{GJ} in hand, we moved on to determine the methanol oxidation activity. For decades, an artificial dye-coupled assay that utilizes redox-active dyes has been widely employed to assess the enzyme activity of MDHs derived from a vast variety of microorganisms.[1a,7,22] In addition to the non-specificity of the dye-coupled assay to MDH, the commercially available and low-cost reagents favor the usage of this assay. However, this method does not mirror the mechanism *in vivo* and conclusions drawn from the dye-coupled assay should be considered carefully. PES/DCPIP and the alternative dye-coupled method with Wurster's Blue are all photosensitive, can induce high background reactivity and should be performed vigilantly.[18b] Similar to previous work, the specific activity of the Ln-MDHs with early Lns is higher and increases towards Nd-MDH and then decline subsequently (Figure 2A). In order to account for the varying metal content among samples, we adjusted the specific activities by assuming a 100% metal content within the active site. Due to the relatively low metal content of Tb (11.3%) in the MDH sample purified from cells grown on Tb and likely even lower metalation of the active site and activation of PQQ, the adjusted specific activity is likely to be artificially inflated, but was included for transparency. For the smaller Lns, several theoretical studies have shown that the activation of PQQ is insufficient, preventing effective oxidation.[10a,23] The low metalation of the sample leads to a substantial increase in uncertainty and will not be further discussed. Earlier studies obtained and compared the activity of different XoxF-MDHs by titrating the desired Ln to partial-apo Eu-MDH or incubating apo-MDH with Ln and PQQ.[7,10a,12a,22] To the best of our knowledge, the isolation of various Ln-MDHs from a microorganism grown with its respective Ln has not been widely practiced so far. Singer *et al.* were able to receive XoxF-MDH containing the heavier, smaller Lns by expressing an apo-XoxF-MDH in *Escherichia coli* and incubation with the respective Ln and PQQ for 72 hours.[12a] The results of their dye-coupled activity assays show that Tb-MDH is less active than Gd-MDH (although it should be noted, that metalation was not investigated here).

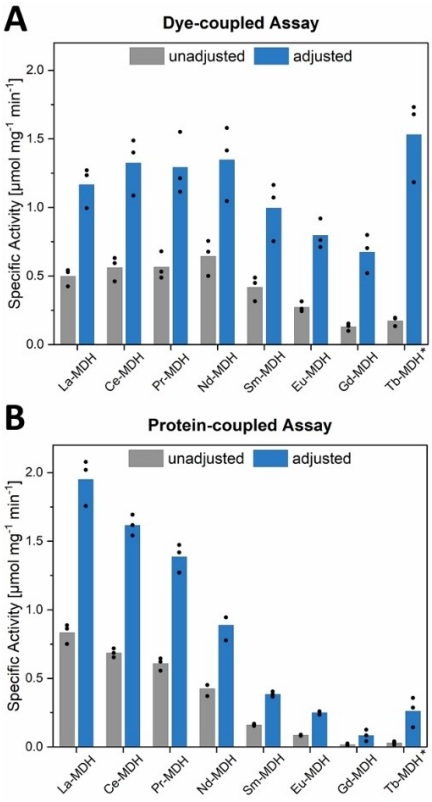

Figure 2. Results of the determination of specific enzyme activity using (A) the dye-coupled and (B) protein-coupled assay (outlined in Figure 1B). Conditions dye-coupled assay: 100 nM XoxF-MDH, 1 mM PES, 100 µM DCPIP, 50 mM MeOH in 10 mM PIPES with 1 mM MeOH, pH 7.2, 45 °C. Conditions protein-coupled assay: 100 nM XoxF-MDH, 5 µM cyt c_{GJ}, 50 µM cyt *c* from equine heart, 50 mM MeOH in 10 mM PIPES with 1 mM MeOH, pH 7.2, 45 °C. The adjusted values are calculated assuming 100% metal content in the active site. Technical replicates (n = 3) were conducted and each dot represents the result of one measurement. *The relatively low metal content of Tb-MDH (11.3%) likely inflates the adjusted value for the enzymatic activity.

Computational and experimental studies also discuss the effect of the Lewis acidity of the Ln on enzyme activity.[7,10a–c] Due to the Ln contraction, the Lewis acidity increases across the Ln series. PQQ requires a Lewis acid to activate its C5 quinone C–O bond for the subsequent proton abstraction step of the substrate. Higher Lewis acidity facilitates the rate-limiting breaking of the substrate C–H bond hence increasing substrate turnover and enzyme activity but obtaining XoxF-MDH with late Ln remains challenging.

A protein-coupled activity assay is another method to investigate kinetic parameters of MDHs. Anthony and coworkers developed a protein-coupled activity assay for MxaFI-MDH from *M. extorquens* AM1.[19,24] The assay mixture is composed of MxaFI-MDH, its physiological partner cyt c_L, cyt *c* from equine or bovine heart and MeOH as substrate. The physiological electron acceptor cyt c_L is used to re-oxidize MxaFI-MDH and the introduction of the secondary cytochrome *c* from equine or bovine heart is able to re-oxidze cyt c_L without interacting with MDH (Figure 1B).[24] Versantvoort *et al.* have shown with XoxF-MDH from SolV that the rate of reduction of the secondary cytochrome depends on the concentration of the physiological partner cytochrome which appeared to be linear between 0 and 1 µM for cyt c_{GJ}.[15] This method reflects the physiological mechanism more accurately and is easier to handle without photosensitive reagents. A limitation is the MDH-specificity of the real physiological cytochrome partners although some rare cases are reported where this was still possible, e.g. the cyt c_L of AM1 is able to interact with MDH from *Paracoccus denitrificans* and *Methylophilus methylotrophus*.[24] Featherston *et al.* discussed the subtle differences of the immediate cytochromes MxaG and XoxG of MxaFI-MDH and XoxF-MDH, respectively, from *M. extorquens* AM1.[17] Both cytochromes are *c*-type cytochromes and carry the typical characteristics: covalent attachment of the heme *c* moiety to the protein *via* two thioether bonds and axial ligation of the Fe^{3+} by histidine and a second, in this case, a methionine residue.[25] The main distinctions are the loss of a helix in cyt *c* XoxG and the absence of a Ca^{2+} binding site in another helix. These differences result in more solvent-exposed heme that is

proposed to be the source of the relatively low midpoint reduction value of the XoxG-type cytochromes.[17] These subtle yet important structural changes are likely to result in different enzymatic activity of MDHs *in vivo* and cannot be properly reflected by an artificial dye-coupled assay. Thus, conclusions deduced from dye-coupled assays should be drawn carefully.

The highly laborious work to obtain adequate protein quantities required for protein-coupled activity assays is another hindrance, which should be considered. Before we conduct protein-coupled assay of XoxF-MDHs with cyt c_{GJ}, we determined the optimal concentration of cyt c_{GJ} to obtain maximum substrate turnover. Among all tested Ln-MDHs, Nd-MDH demonstrated the highest enzyme activity based on the dye-coupled assay and was chosen as the proxy for this experiment. Nd-MDH was assayed with increasing amount of cyt c_{GJ} (0–30 μM) and Michaelis-Menten kinetics were obtained by best curve fitting (Figure S4).

Based on these results, a concentration of cyt c_{GJ} above 100 μM is required to obtain v_{max}, which is a prohibitively large amount of cyt c_{GJ} for a single assay. Therefore, we decided to choose a value at the end of the linear phase and proceeded with 5 μM cyt c_{GJ} for each assay. We evaluated the enzymatic activity of eight XoxF-MDHs with the protein-coupled assay and the results are shown in Figure 2B. In order to exclude any day-to-day deviation, we used the same enzyme batch for both methods and conducted the experiments on the same day. In contrast to the dye-coupled assay, we observed a gradual decrease in enzymatic activity across the Ln series. Again, Gd-MDH displays the lowest enzyme activity, while La-MDH exhibits the highest enzyme activity. Regardless of method, Gd-MDH constantly remains the least active MDH. As discussed above, Lewis acidity can have a significant impact on substrate turnover through various mechanisms. Additional functions of the Lewis acid, like substrate orientation, cofactor redox cycling and substrate activation and their effects on the enzyme activity, have been discussed.[10a,c,d,26] We found that the specific enzyme activity of La-, Ce- and Pr-MDH is higher with the protein-coupled assay compared to their activity measured with the dye-coupled assay. In contrast, Nd-, Sm-, Eu- and Gd-MDH exhibit lower specific activity with the protein-coupled assay than with the dye-coupled assay. These results indicate that, depending on the assay, distinct trends can be observed among the XoxF-MDHs, implying that different aspects of the enzyme activity are being measured. Moreover, the protein-coupled assay revealed greater specific enzyme activity for La-, Ce- and Pr-MDH suggesting that these Lns may positively affect the efficiency in cyt c_{GJ} reduction. In comparison to the dye-coupled assay, protein-protein interaction steps are involved in the protein-coupled assay to transfer the electrons from XoxF-MDH to the final electron acceptor, but the positive effect of La, Ce and Pr on the interaction still exceed this challenge. These results indicate that La, Ce and Pr are not just suitable Lewis acids that catalyze the rate-limiting step for substrate turnover, but also facilitate and enhance the electron transfer between XoxF-MDH and its cyt c_{GJ}, thereby increasing the overall functional efficiency. We cannot rule out that the use of 5 μM cyt c_{GJ} may not be optimal and might be sufficient to reach v_{max} for one XoxF-MDH but not for another such as Nd-MDH.

Conclusions

To conclude, we have grown *M. fumariolicum* SolV with nine different Lns and were able to purify eight different XoxF-MDHs, and their physiological electron acceptor cyt c_{GJ} and assessed the enzyme activity by performing dye- and protein-coupled activity assays. ICP-MS measurements revealed that XoxF-MDH contain varying amount of Ln in their active site and that this value decreases towards Tb. ICP-MS also showed that XoxF-MDH isolated from Lu-grown SolV was not able to incorporate any Lu. Next, we determined the enzyme activity using the dye-coupled assay with PES/DCPIP and compared the results with the protein-coupled assay using cyt c_{GJ} as electron acceptor. The data obtained from each method showed a discernible and distinct pattern Ln-MDHs, providing evidence that these methods are impacted by different aspects of the Ln-dependent enzyme activity. Both methods revealed that Gd-MDH is the least active among the eight XoxF-MDHs and that the enzymes containing larger Lns have higher activity, but different trends amongst the Ln series are observed based on the method used. At first glance, the increased activity of XoxF-MDH with early Lns align with the higher growth rates of SolV when cultivated with early Lns, suggesting that the growth of SolV is mainly linked to the activity of XoxF-MDH.[6,12a] Wegner and co-workers discovered in *Beijerinckiaceae* bacterium RH AL1 that the addition of La or a Ln cocktail change the expression of nearly 41% of all genes in the genome and that different Lns affect different genes. Differentially expressed genes are associated with various biological processes of the Ln-dependent metabolism but also include secretion and uptake system, the flagellar and chemotactic machinery and other cellular functions.[27] Therefore, the influence of Lns extend beyond their catalytic role in methanol oxidation.

Using the dye-coupled assay, the enzyme activity increases towards Nd-MDH and declines afterwards. These results are in accordance with previous studies.[7,10a,12a,22] Using the protein-coupled assay, La-MDH displayed the highest enzyme activity which decreases progressively towards Gd-MDH. Although more steps are involved to transfer the electrons from XoxF-MDH to the final electron acceptor, we observed that La-, Ce- and Pr-MDH exhibit higher enzymatic activity in the protein-coupled assay than in the dye-coupled assay. This indicates that the enhancing effects of Ln are not limited to XoxF-MDH but also influence the electron transfer by its cyt c_{GJ}. When adjusting the enzyme activity by their varying metal content, the trends became more pronounced, supporting our findings. This normalization allowed us to account for any potential discrepancies in the metal content and increases the accuracy and reliability of the results. To enhance reproducibility and comparability, we propose to incorporate the determination of metal content by ICP-MS into any kinetic experiments that involves metalloenzymes. This additional step will ensure that

variations in metal content are accounted for, which will enable more meaningful comparisons between different experiments.

Experimental Section

Bacterial culture

The cultivation of *M. fumariolicum* SolV (La–Eu) was performed by using a modified protocol as previously reported.[12a] For the composition of the growth medium see Table S1. SolV was grown with the desired Ln (La–Eu) in single-use polypropylene plastic cultivation flasks to an optical density at 600 nm (OD_{600}) of 0.5. Around 100–200 mL of SolV culture was used to inoculate the large-scale (3.5 L) bioreactor (non-commercial, self-build) to obtain a starting OD_{600} of 0.05.[12b] Throughout the cultivation, CO_2 (600 mL/min), CH_4 (750 mL/min) and air (1000 mL/min) was sparged through the medium. The temperature was kept at 55 °C and a stirring bar was used to ensure homogeneity and even distribution of gases.

The inoculants for Gd- and Tb-grown SolV were obtained by starvation of La-grown SolV through two cycles:

Minimal medium (100 mL) and La-grown SolV was added to a 1 L cultivation flask to a starting OD_{600} of 0.05. For incubation, a gas atmosphere of 85% air, 10% CH_4 and 5% CO_2 was provided. The flask was incubated in a shaker at 55 °C and 250 rpm for 4 days until an OD_{600} of around 0.25 was reached (cycle 1). 100 mL of this starved La-grown SolV was used to repeat the same procedure once more until an OD_{600} of 0.125 was reached (cycle 2). In the third round, 100 nM $GdCl_3$ or $TbCl_3$ was added to the starved SolV culture and further incubated until the desired OD_{600} was reached and then used as inoculant for the bioreactor.

Protein Purification

M. fumariolicum SolV cells were harvested by centrifugation at 8000 rpm for 10 min (Avanti JXN-26, Beckman Coulter). The cells were resuspended in 10 mM PIPES (piperazine-*N*,*N*′-bis(2-ethanesulfonic acid) supplemented with 1 mM MeOH (pH 7.2) and chemically lysed by commercially available BugBuster Protein Extraction Reagent (Merck, product code 70921). 10xBugBuster Protein Extraction Reagent was diluted to 1x with 10 mM PIPES and 1 mM MeOH (pH 7.2). The reagent was added to frozen or thawed cell pellet (2 mL 1xBugBuster per 1 g resuspended cells), followed by the addition of 0.5–1.0 mg/mL lysozyme from chicken egg white (Sigma-Aldrich, CAS 12650–88-3), 0.2–0.5 mg/mL DNase I (PanReac AppliChem, product code A3778,0100) and incubated on a shaking platform for 30–45 min at room temperature. Afterwards, insoluble cell debris were removed by centrifugation (17000 rpm, 20 min, 4 °C). After filtration of the supernatant with a filter paper (VWR, 5–13 μm particle retention), the sample was applied on a HiPrep™ SP Sepharose FF 16/10 cation exchange column (Cytiva, product code 28936544). The column was equilibrated with 10 mM PIPES with 1 mM MeOH (pH 7.2) and bound proteins were eluted using 10 mM PIPES with 1 M NaCl and 1 mM MeOH (pH 7.2). Cyt c_{GJ} eluted at 2% (20 mM NaCl) and MDH at 25% (250 mM NaCl). Cyt c_{GJ} was further concentrated using an Amicon® Ultra Centrifugal Unit (Merck, product code UFC901024) with a molecular weight cut-off of 10 kDa and applied on a HiLoad™ 16/600 Superdex™ 75 pg size exclusion column (Cytiva, product code 28989333). The column was equilibrated with 10 mM PIPES and 0.2 M NaCl (pH 7.2) and cyt c_{GJ} started to elute after 65 mL at a flowrate of 0.3 mL/min recording the UV/Vis absorption at 280 nm and its Soret peak of 434 nm. The NaCl concentration was reduced to less than 1 mM with an Amicon® Ultra Centrifugal Unit (Merck, UFC201024) with a molecular weight cut-off of 10 kDa and 10 mM PIPES (pH 7.2).

For SDS-PAGE analysis, mPAGE® 4X LDS sample buffer (Merck, product code MPSB-10 ML) containing 2% β-mercaptoethanol was added to samples and then heated at 70 °C for 5–7 min. The samples were loaded on a 12% SDS-PAGE gel (12% w/v acrylamide). The gel was stained with Coomassie Blue Stain for 1 h and subsequently treated with a destaining solution (10% (v/v) acetic acid and 20% (v/v) EtOH in ultrapure water). MDHs (63.5 kDa) and cyt c_{GJ} (29.7 kDa) appear as dominant bands (Figure S3).

Activity Assays

The activity assay with cyt c_{GJ} and artificial electron acceptors are based on the protocols reported by Gutenthaler *et al.*[8] The enzymatic activity of MDH was assessed with native cyt c_{GJ} through the reduction of equine heart cyt *c* (Sigma, CAS 9007-43-6). The reaction was monitored with an Epoch2 plate reader (formerly BioTek, now Agilent) at 45 °C through the increase of A_{550}. All experiments were conducted in 96-well-plates. Each well contained a total volume of 100 μL with 50 μM equine heart cytochrome *c*, 5 μM cyt c_{GJ}, 100 nM MDH and 50 mM MeOH in 10 mM PIPES with 1 mM MeOH (pH 7.2). Everything but MDH were mixed together and incubated for 2 min at 45 °C before the reaction was initiated with the addition of MDH which was also incubated for 2 min at 45 °C. The extinction coefficient of equine heart cytochrome *c* was previously determined at 19.5 $mM^{-1}\,cm^{-1}$ for 10 mM PIPES (pH 7.2).[15] The specific activity was calculated using the slope of the initial 2 min after MDH addition. The specific activity of each experiment was adjusted according to the metal content of the MDH.

$$enzyme\ unit\ U\ [\mu mol\ min^{-1}] = \frac{initial\ rate\ of\ slope\ of\ measurement}{\varepsilon\ [cm^{-1}\ M^{-1}] \times pathlength\ of\ cell\ [cm]} \times 10^6 \times volume\ of\ assay\ [L]$$

$$specific\ activity\ [\mu mol\ min^{-1}\ mg^{-1}] = \frac{enzyme\ Unit\ U\ [\mu mol\ min^{-1}]}{amount\ of\ enzyme\ [mg]}$$

$$specific\ activity_{adjusted}\ [\mu mol\ min^{-1}\ mg^{-1}] = \frac{enzyme\ Unit\ U\ [\mu mol\ min^{-1}]}{amount\ of\ enzyme\ [mg] \times \frac{metal\ content\ [\%]}{100}}$$

The activity assay with the artificial electron acceptor DCPIP (2,6-Dichlorophenolindophenol sodium salt dihydrate, formerly Fluka, now Honeywell, CAS: 1266615–56-8) and PES (phenazine ethosulfate, Sigma-Aldrich, CAS 10510-77-7) was assessed through the reduction of DCPIP. The reaction was monitored with an Epoch2 plate reader (formerly BioTek, now Agilent) through the decrease of A_{600}. Each well contained a total volume of 100 μL with 1 mM PES, 100 μM DCPIP, 100 nM MDH, 50 mM MeOH in 10 mM PIPES with 1 mM MeOH (pH 7.2). Everything but MDH were mixed and incubated for 2 min at 45 °C in the dark before the reaction was initiated with addition of MDH which was also incubated for 2 min at 45 °C in the dark. The extinction coefficient of DCPIP was determined at 19.8 $mM^{-1}\,cm^{-1}$ for 10 mM PIPES (pH 7.2). The specific activity was calculated using the slope of the initial 2 min

after MDH addition. The specific activity of each experiment was adjusted according to the metal content of the MDH.

$$enzyme\ unit\ U\ [\mu mol\ min^{-1}] = \frac{-1 \times initial\ rate\ of\ slope\ of\ measurement}{\varepsilon\ [cm^{-1}\ M^{-1}] \times pathlength\ of\ cell\ [cm]} \times 10^{6} \times volume\ of\ assay\ [L]$$

$$specific\ activity\ [\mu mol\ min^{-1}\ mg^{-1}] = \frac{enzyme\ Unit\ U\ [\mu mol\ min^{-1}]}{amount\ of\ enzyme\ [mg]}$$

$$specific\ activity_{adjusted}\ [\mu mol\ min^{-1}\ mg^{-1}] = \frac{enzyme\ Unit\ U\ [\mu mol\ min^{-1}]}{amount\ of\ enzyme\ [mg] \times \frac{metal\ content\ [\%]}{100}}$$

The Michaelis-Menten constant K_M and the maximum turnover speed v_{max} of the cyt c_{GJ}-based activity assay (0–30 μM) with 100 nM Nd-MDH were calculated with the Michaelis-Menten equation using the slope of the initial 2 min after initiation:

$$v_0 = \frac{v_{max}[S]}{K_M + [S]}$$

With v_0 representing the initial velocity and [S] the substrate concentration. The specific activity of each experiment was adjusted according to the metal content of Nd-MDH (47.8%).

Metal analysis by ICP-MS

The Ln-content of each MDH was determined by addition of the samples to 3% nitric acid (Suprapur®, Supelco) and heating for 1 h at 90 °C before analysis using an Inductively Coupled Plasma Mass Spectrometer (Nexion 350D, Perkin Elmer). Protein concentration were determined spectrophotometrically at 280 nm using an extinction coefficient of 158 cm^{-1} mM^{-1}.[6] The metal content of the Ln-MDHs (technical duplicates) used in these experiments was determined at 42.7% for La-MDH, 42.4% for Ce-MDH, 43.8% for Pr-MDH, 47.8% for Nd-MDH, 41.9% for Sm-MDH, 34.3% for Eu-MDH, 19.2% for Gd-MDH and 11.3% for Tb-MDH.

Acknowledgements

The authors thank Christine Benning for ICP-MS measurements. We thank Dr. Arjan Pol for his input on SolV cultivation. SS, MTP and LJD acknowledge support from the Deutsche Forschungsgemeinschaft (DFG) projects 325871075 (SFB1309), 392552271 and SCHN1273-5. Open Access funding enabled and organized by Projekt DEAL.

Conflict of Interests

The authors declare no conflict of interest.

Data Availability Statement

Further data available in the SI.

Keywords: lanthanide-dependent bacteria · lanthanides · methanol dehydrogenase · methylotrophy · metalloenzymes

[1] a) T. Nakagawa, R. Mitsui, A. Tani, K. Sasa, S. Tashiro, T. Iwama, T. Hayakawa, K. Kawai, *PLoS One* **2012**, *7*, e50480; b) S. Kato, M. Takashino, K. Igarashi, W. Kitagawa, *Microbes Environ.* **2020**, *35*; c) B. Vekeman, D. Speth, J. Wille, G. Cremers, P. De Vos, H. J. M. Op den Camp, K. Heylen, *Microb. Ecol.* **2016**, *72*, 503–509; d) M. Taubert, C. Grob, A. M. Howat, O. J. Burns, J. L. Dixon, Y. Chen, J. C. Murrell, *Environ. Microbiol.* **2015**, *17*, 3937–3948; e) H. Lv, N. Sahin, A. Tani, *Environ. Microbiol.* **2018**, *20*, 1204–1223; f) P. Roszczenko-Jasińska, T. Krucoń, R. Stasiuk, R. Matlakowska, *FEMS Microbiol. Ecol.* **2020**, *97*; g) S. Hou, K. S. Makarova, J. H. W. Saw, P. Senin, B. V. Ly, Z. Zhou, Y. Ren, J. Wang, M. Y. Galperin, M. V. Omelchenko, Y. I. Wolf, N. Yutin, E. V. Koonin, M. B. Stott, B. W. Mountain, M. A. Crowe, A. V. Smirnova, P. F. Dunfield, L. Feng, L. Wang, M. Alam, *Biol. Direct* **2008**, *3*, 26.
[2] L. Chistoserdova, *Environ. Microbiol.* **2011**, *13*, 2603–2622.
[3] a) H. In Yeub, L. Seung Hwan, C. Yoo Seong, P. Si Jae, N. Jeong Geol, C. In Seop, K. Choongik, K. Hyun Cheol, K. Yong Hwan, L. Jin Won, *J. Microbiol. Biotechnol.* **2014**, *24*, 1597–1605; b) A. S. Hakemian, A. C. Rosenzweig, *Annu. Rev. Biochem.* **2007**, *76*, 223–241; cT. J. Kang, E. Y. Lee, *J. Ind. Eng. Chem.* **2016**, *35*, 8–13.
[4] a) R. A. Schmitz, N. Picone, H. Singer, A. Dietl, K.-A. Seifert, A. Pol, M. S. M. Jetten, T. R. M. Barends, L. J. Daumann, H. J. M. O. d. Camp, M. W. Ribbe, *mBio* **2021**, *12*, e01708–01721; b) L. Chistoserdova, M. G. Kalyuzhnaya, *Trends Microbiol.* **2018**, *26*, 703–714.
[5] a) C. Mackenzie, M. Choudhary, F. W. Larimer, P. F. Predki, S. Stilwagen, J. P. Armitage, R. D. Barber, T. J. Donohue, J. P. Hosler, J. E. Newman, J. P. Shapleigh, R. E. Sockett, J. Zeilstra-Ryalls, S. Kaplan, *Photosynth. Res.* **2001**, *70*, 19–41; b) G. Bosch, T. Wang, E. Latypova, M. G. Kalyuzhnaya, M. Hackett, L. Chistoserdova, *Microbiology* **2009**, *155*, 1103–1110.
[6] A. Pol, T. R. M. Barends, A. Dietl, A. F. Khadem, J. Eygensteyn, M. S. M. Jetten, H. J. M. Op den Camp, *Environ. Microbiol.* **2014**, *16*, 255–264.
[7] B. Jahn, A. Pol, H. Lumpe, T. R. M. Barends, A. Dietl, C. Hogendoorn, H. J. M. Op den Camp, L. J. Daumann, *ChemBioChem* **2018**, *19*, 1147–1153.
[8] S. M. Gutenthaler, M. T. Phi, H. Singer, L. J. Daumann, in *Methods Enzymology, Vol. 650* (Ed.: J. A. Cotruvo), Academic Press, **2021**, pp. 57–79.
[9] a) H. N. Vu, G. A. Subuyuj, S. Vijayakumar, N. M. Good, N. C. Martinez-Gomez, E. Skovran, *J. Bacteriol.* **2016**, *198*, 1250–1259; b) F. Chu, M. E. Lidstrom, *J. Bacteriol.* **2016**, *198*, 1317–1325; c) W. Gu, M. Farhan Ul Haque, A. A. DiSpirito, J. D. Semrau, *FEMS Microbiol. Lett.* **2016**, *363*; d) S. Masuda, Y. Suzuki, Y. Fujitani, R. Mitsui, T. Nakagawa, M. Shintani, A. Tani, *mSphere* **2018**, *3*, 10.1128/msphere.00462-00417.
[10] a) H. Lumpe, A. Pol, H. J. M. Op den Camp, L. J. Daumann, *Dalton Trans.* **2018**, *47*, 10463–10472; b) M. Prejanò, N. Russo, T. Marino, *Chem. Eur. J.* **2020**, *26*, 11334–11339; c) M. Prejanò, T. Marino, N. Russo, *Chem. Eur. J.* **2017**, *23*, 8652–8657; d) M. Leopoldini, N. Russo, M. Toscano, *Chem. Eur. J.* **2007**, *13*, 2109–2117; e) C. Anthony, *Arch. Biochem. Biophys.* **2004**, *428*, 2–9.
[11] A. Pol, K. Heijmans, H. R. Harhangi, D. Tedesco, M. S. M. Jetten, H. J. M. Op den Camp, *Nature* **2007**, *450*, 874–878.
[12] a) H. Singer, R. Steudtner, A. S. Klein, C. Rulofs, C. Zeymer, B. Drobot, A. Pol, N. C. Martinez-Gomez, H. J. M. Op den Camp, L. Daumann, *Angew. Chem. Int. Ed.* **2023**, *62*, e202303669; b) H. Singer, R. Steudtner, I. Sottorff, B. Drobot, A. Pol, H. J. M. Op den Camp, L. J. Daumann, *Chem. Commun.* **2023**, *59*, 9066–9069.
[13] C. Anthony, *Biochim. Biophys. Acta* **1992**, *1099*, 1–15.
[14] a) J. M. Cox, D. J. Day, C. Anthony, *Biochim. Biophys. Acta* **1992**, *1119*, 97–106; b) C. Anthony, in *Enzyme-Catalyzed Electron and Radical Transfer: Subcellular Biochemistry* (Eds.: A. Holzenburg, N. S. Scrutton), Springer US, Boston, **2000**, pp. 73–117; c) P. R. Afolabi, F. Mohammed, K. Amaratunga, O. Majekodunmi, L. Dales, R. Gill, D. Thompson, B. Cooper, P. Wood, M. Goodwin, C. Anthony, *Biochemistry* **2001**, *40*, 9799–9809.
[15] W. Versantvoort, A. Pol, L. J. Daumann, J. A. Larrabee, A. H. Strayer, M. S. M. Jetten, L. van Niftrik, J. Reimann, H. J. M. Op den Camp, *Biochim. Biophys. Acta* **2019**, *1867*, 595–603.

[16] P. Kalimuthu, L. J. Daumann, A. Pol, H. J. M. Op den Camp, P. V. Bernhardt, *Chem. Eur. J.* **2019**, *25*, 8760–8768.
[17] E. R. Featherston, H. R. Rose, M. J. McBride, E. M. Taylor, A. K. Boal, J. A. Cotruvo Jr., *ChemBioChem* **2019**, *20*, 2360–2372.
[18] a) R. Ghosh, J. R. Quayle, *Anal. Biochem.* **1979**, *99*, 112–117; b) B. Jahn, N. S. W. Jonasson, H. Hu, H. Singer, A. Pol, N. M. Good, H. J. M. O. den Camp, N. C. Martinez-Gomez, L. J. Daumann, *J. Biol. Inorg. Chem.* **2020**, 199–212.
[19] D. J. Day, C. Anthony, in *Methods Enzymology, Vol. 188*, Academic Press, **1990**, pp. 210–216.
[20] N. A. Danaf, J. Kretzschmar, B. Jahn, H. Singer, A. Pol, H. J. M. Op den Camp, R. Steudtner, D. C. Lamb, B. Drobot, L. J. Daumann, *Phys. Chem. Chem. Phys.* **2022**, *24*, 15397–15405.
[21] N. M. Good, M. Fellner, K. Demirer, J. Hu, R. P. Hausinger, N. C. Martinez-Gomez, *J. Biol. Chem.* **2020**.
[22] M. Wehrmann, P. Billard, A. Martin-Meriadec, A. Zegeye, J. Klebensberger, X. Zhang, D. K. Newman, *mBio* **2017**, *8*, e00570–00517.
[23] S. Tsushima, *Phys. Chem. Chem. Phys.* **2019**, *21*, 21979–21983.
[24] M. Beardmore-Gray, D. T. O'Keeffe, C. Anthony, *Microbiology* **1983**, *129*, 923–933.
[25] a) I. Bertini, G. Cavallaro, A. Rosato, *Chem. Rev.* **2006**, *106*, 90–115; b) J. Liu, S. Chakraborty, P. Hosseinzadeh, Y. Yu, S. Tian, I. Petrik, A. Bhagi, Y. Lu, *Chem. Rev.* **2014**, *114*, 4366–4469.
[26] a) C. Anthony, P. Williams, *Biochim. Biophys. Acta Proteins Proteomics* **2003**, *1647*, 18–23; b) J. A. Bogart, A. J. Lewis, E. J. Schelter, *Chem. Eur. J.* **2015**, *21*, 1743–1748.
[27] a) C.-E. Wegner, M. Westermann, F. Steiniger, L. Gorniak, R. Budhraja, L. Adrian, K. Küsel, *Appl. Environ. Microbiol.* **2021**, *87*, e03144–03120; b) < L. Gorniak, J. Bechwar, M. Westermann, F. Steiniger, C.-E. Wegner, *Microbiol. Spectr.* **2023**, *11*, e00867–823.

Manuscript received: November 30, 2023
Revised manuscript received: December 22, 2023
Version of record online: January 25, 2024